Supporting materials

Mechanistic Insights into the Phase-Directed Green Synthesis of Antibacterial Copper Nanoparticles in Ethaline Deep Eutectic Solvent

Wen Shi,[a] Keshu Song,[a] Shaohua Wang,[a] Zhigang Xu,[b] Xuejiao Zhou,[a] Juan An,[a] Xiaoyan Xiang,[a] Wentang Xia,[a] Wenqiang Yang, [a,b,1]

a School of Metallurgy and Power Engineering, Chongqing University of Science and Technology, Chongqing 401331, P.R. China

b Kopperchem industry Corp., LTD, Solvent Extraction Engineering Research Center, Chongqing 401221, P.R. China

[1] Corresponding author. Tel: +86-023-65023711; Fax: +86-023-65023711.
E-mail address: wenqiangyang@cqust.edu.cn (Wenqiang Yang)

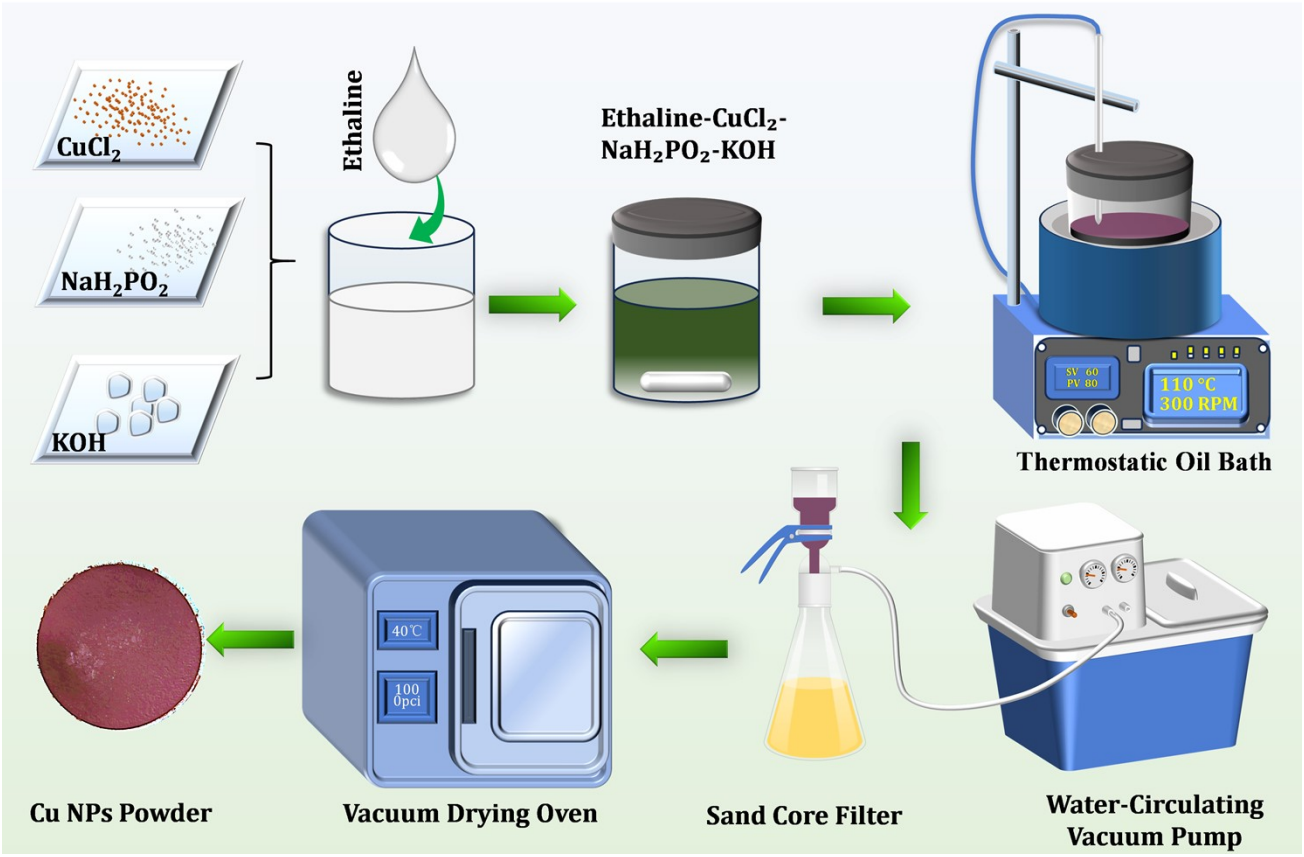

Figure S1. Flowchart of the one-step synthesis of copper nanoparticles in Ethaline deep eutectic solvent.

Figure S2. Photographs of the filter membranes after filtration of the single-solute 0.08 M $CuCl_2$-Ethaline system reacted at different temperatures (353–393 K) for 6 h.

Figure S3. Photographs of the filter membranes after filtration of the binary-solute 0.08 M $CuCl_2$-0.16 M NaH_2PO_2-Ethaline system reacted at different temperatures (353–393 K) for 6 h.

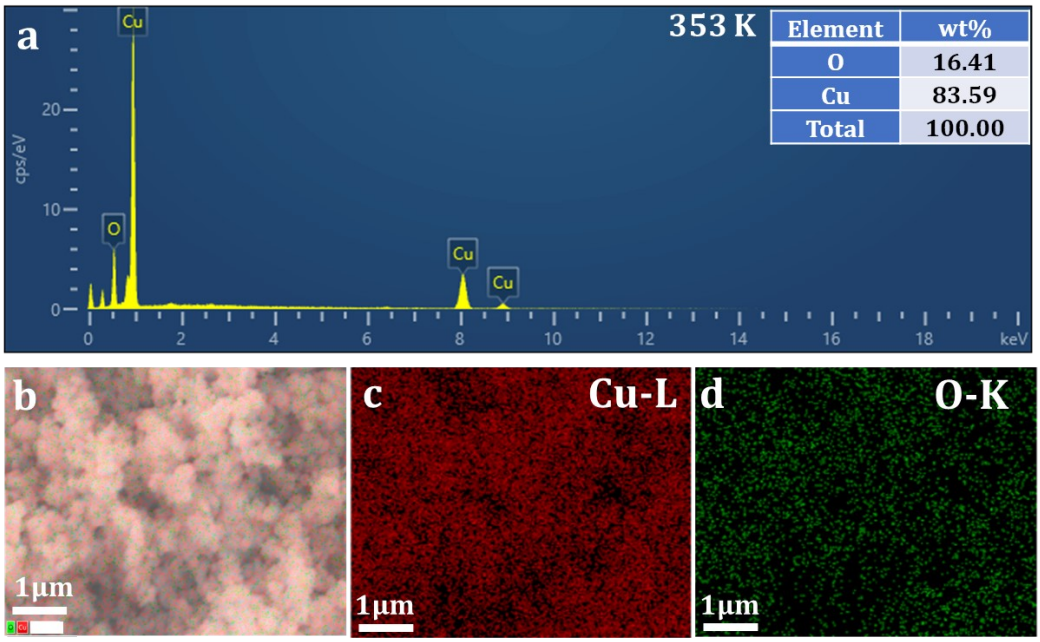

Figure S4. (a) EDS spectrum and (b-d) corresponding elemental distribution maps of the product synthesized in the ternary Ethaline system (0.16 M NaH_2PO_2, 0.24 M KOH, and 0.08 M $CuCl_2$) at 353 K for 6 h.

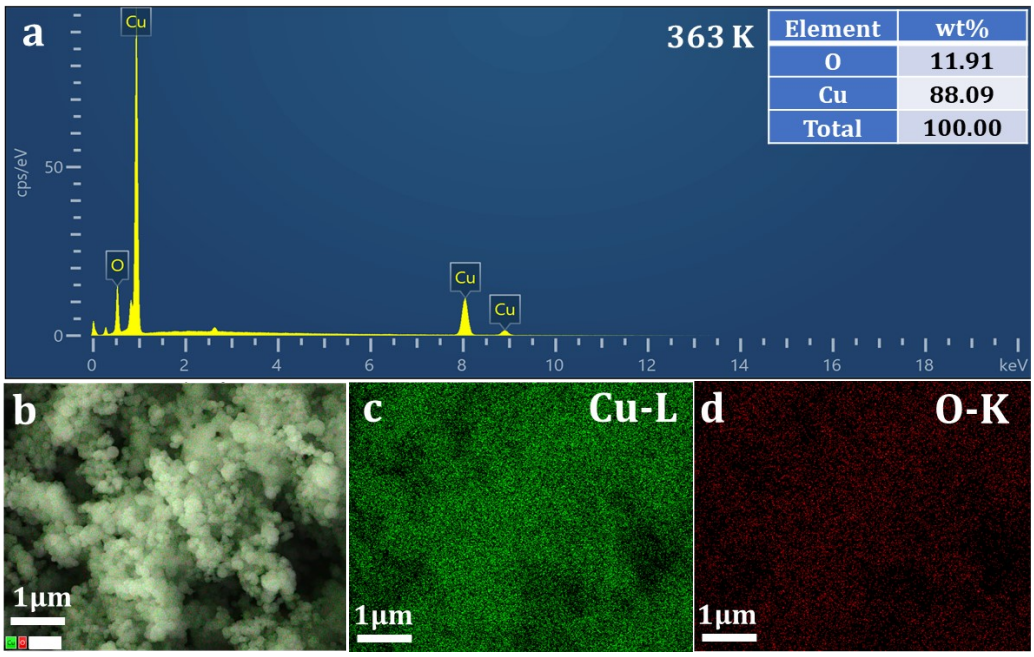

Figure S5. (a) EDS spectrum and (b-d) corresponding elemental distribution maps of the product synthesized in the ternary Ethaline system (0.16 M NaH_2PO_2, 0.24 M KOH, and 0.08 M $CuCl_2$) at 363 K for 6 h.

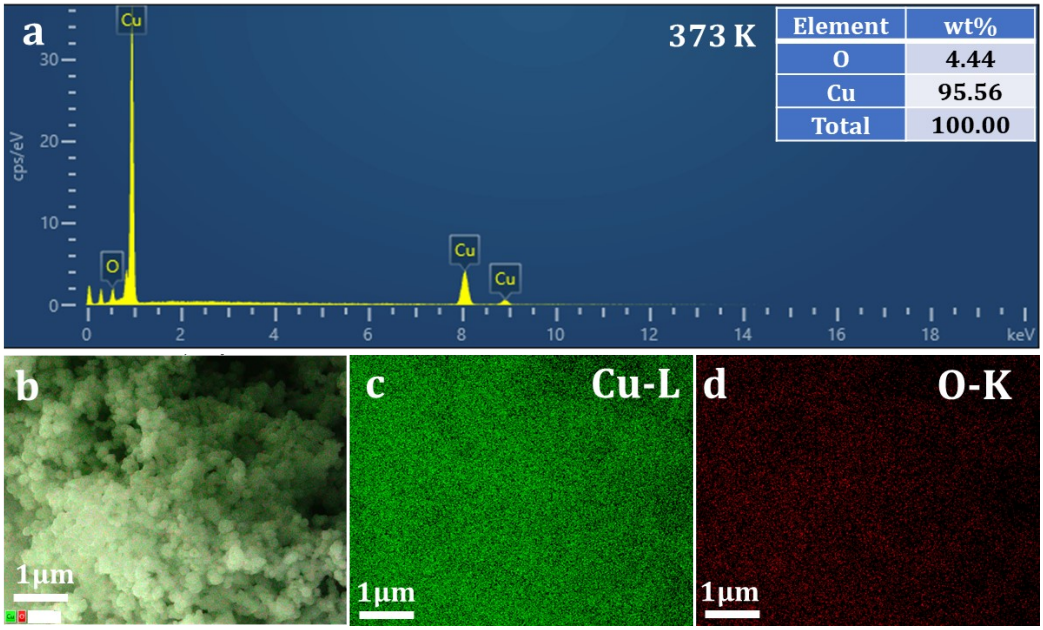

Figure S6. (a) EDS spectrum and (b-d) corresponding elemental distribution maps of the product synthesized in the ternary Ethaline system (0.16 M NaH_2PO_2, 0.24 M KOH, and 0.08 M $CuCl_2$) at 373 K for 6 h.

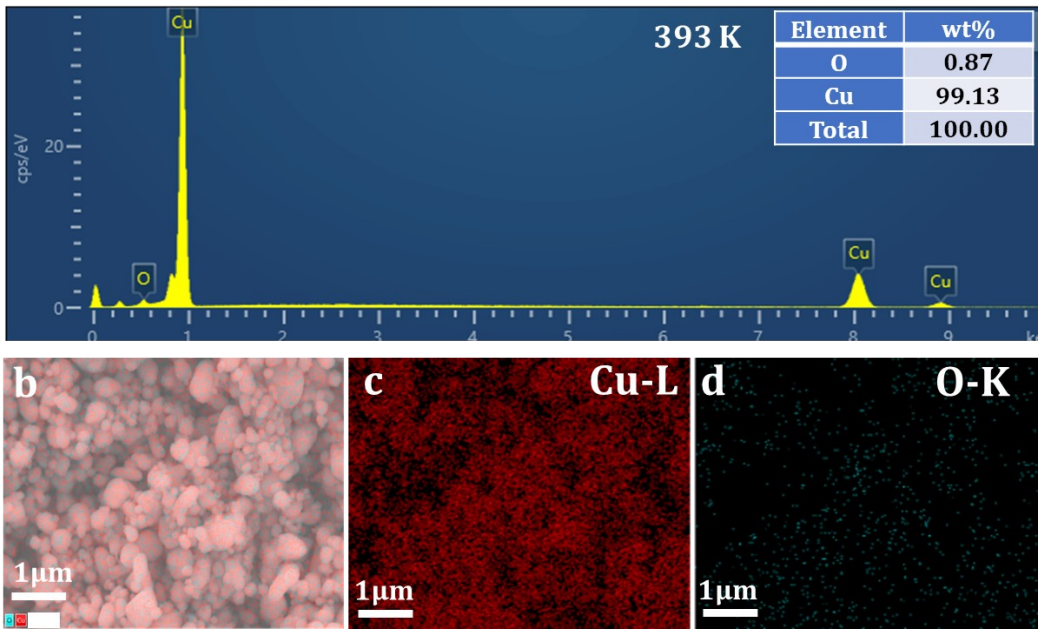

Figure S7. (a) EDS spectrum and (b-d) corresponding elemental distribution maps of the product synthesized in the ternary Ethaline system (0.16 M NaH_2PO_2, 0.24 M KOH, and 0.08 M $CuCl_2$) at 393 K for 6 h.

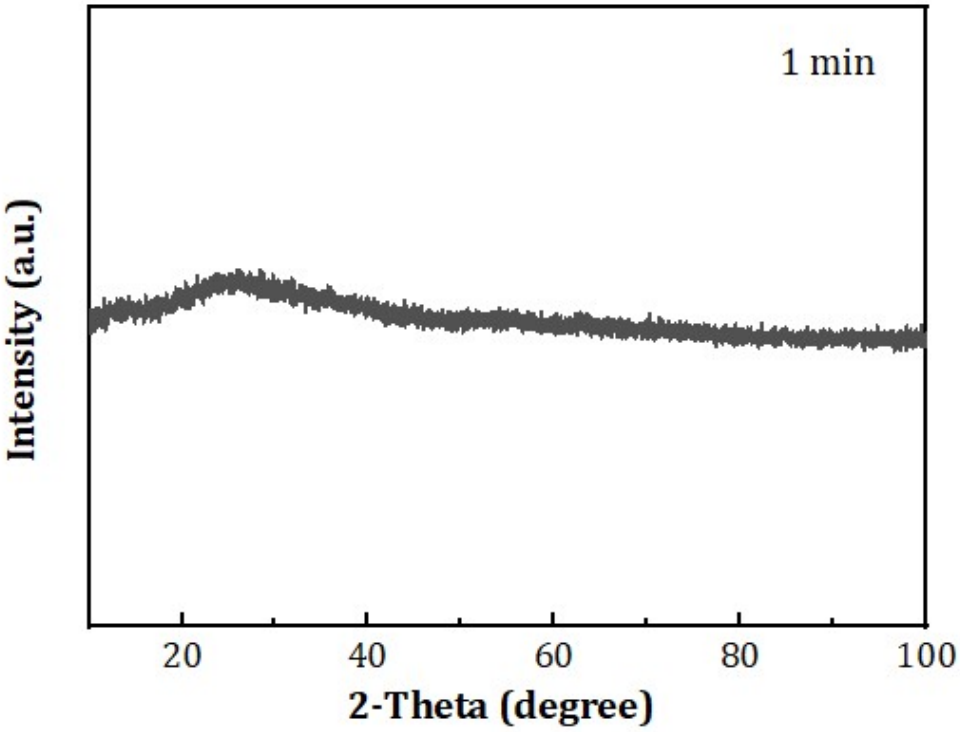

Figure S8. XRD pattern of P-1min.

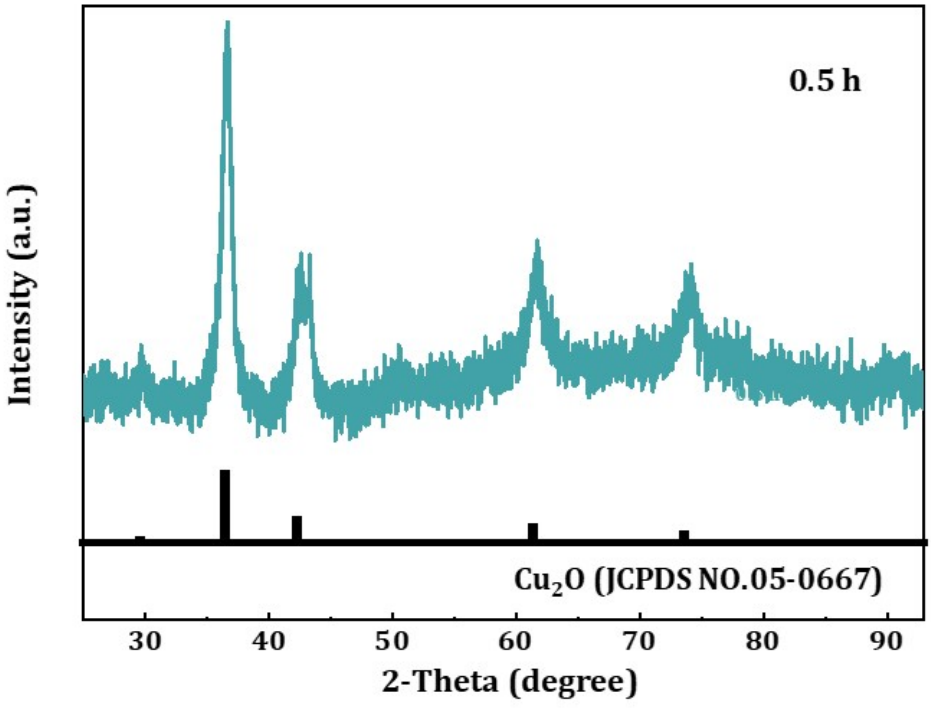

Figure S9. XRD pattern of P-0.5 h sample.

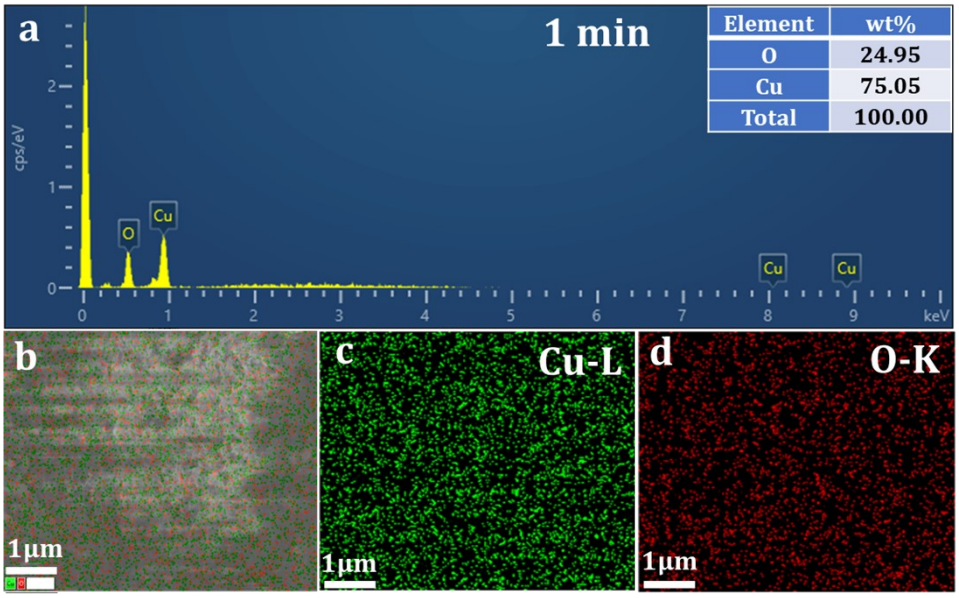

Figure S10. (a) EDS spectrum and (b-d) corresponding elemental distribution maps of P-1min sample.

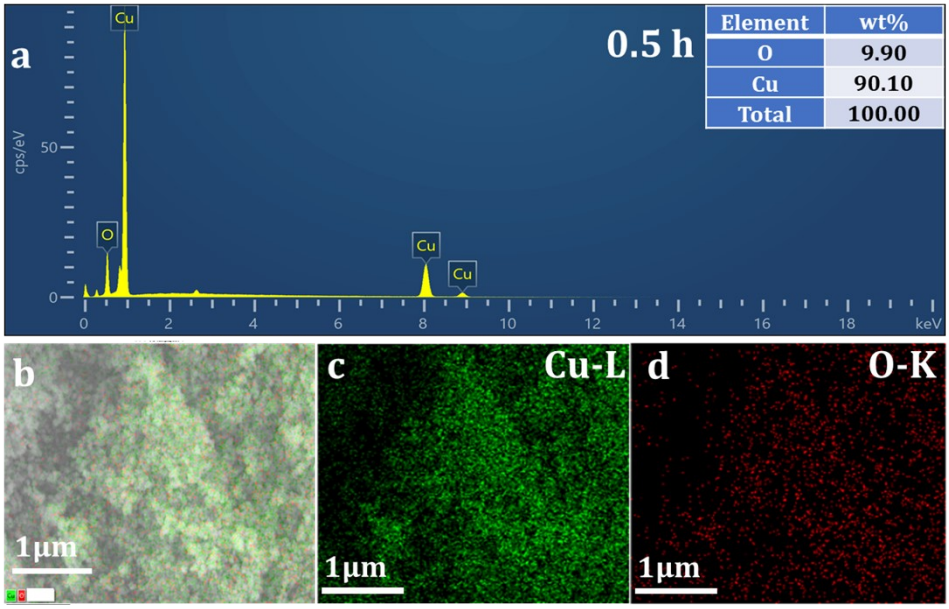

Figure S11. (a) EDS spectrum and (b-d) corresponding elemental distribution maps of P-0.5h sample.

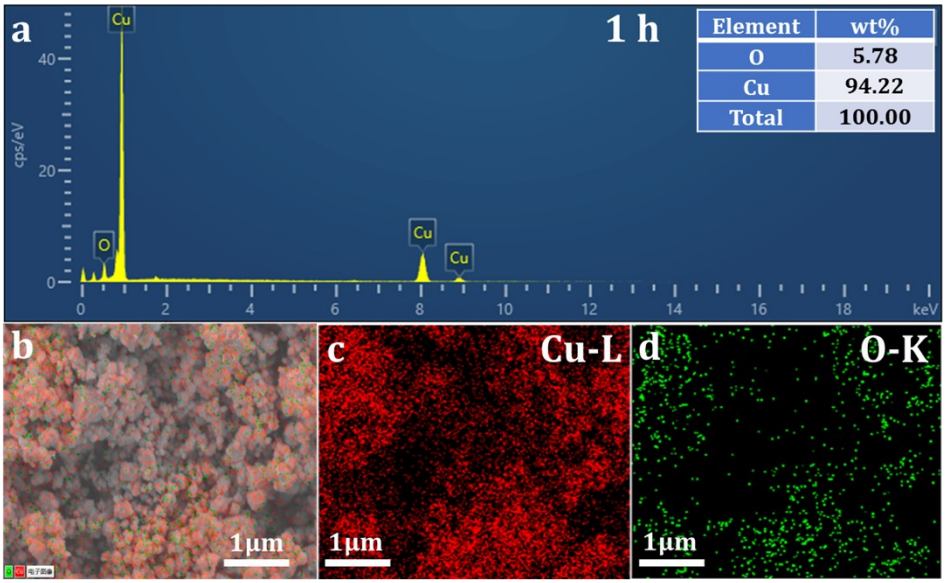

Figure S12. (a) EDS spectrum and (b-d) corresponding elemental distribution maps of P-1h sample.

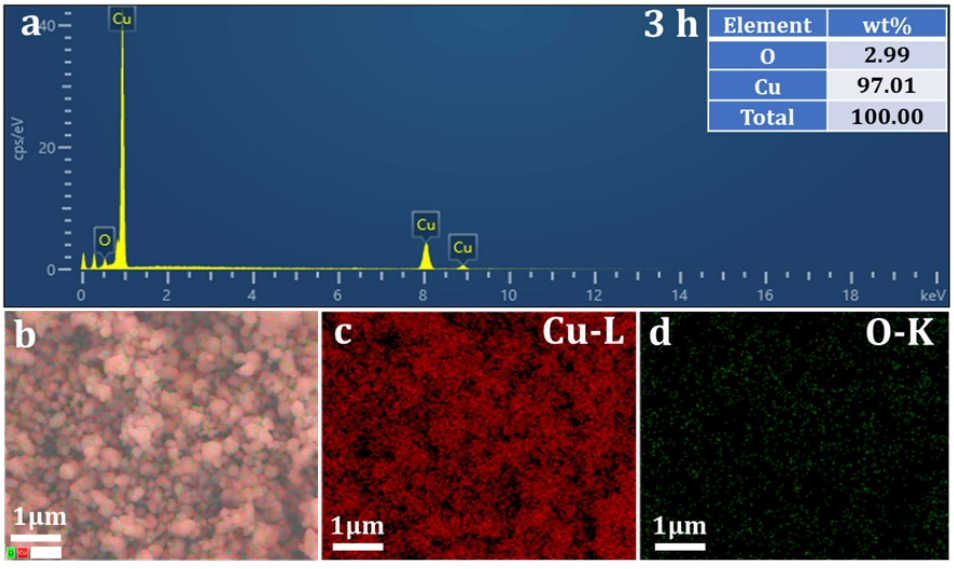

Figure S13. (a) EDS spectrum and (b-d) corresponding elemental distribution maps of P-3h sample.

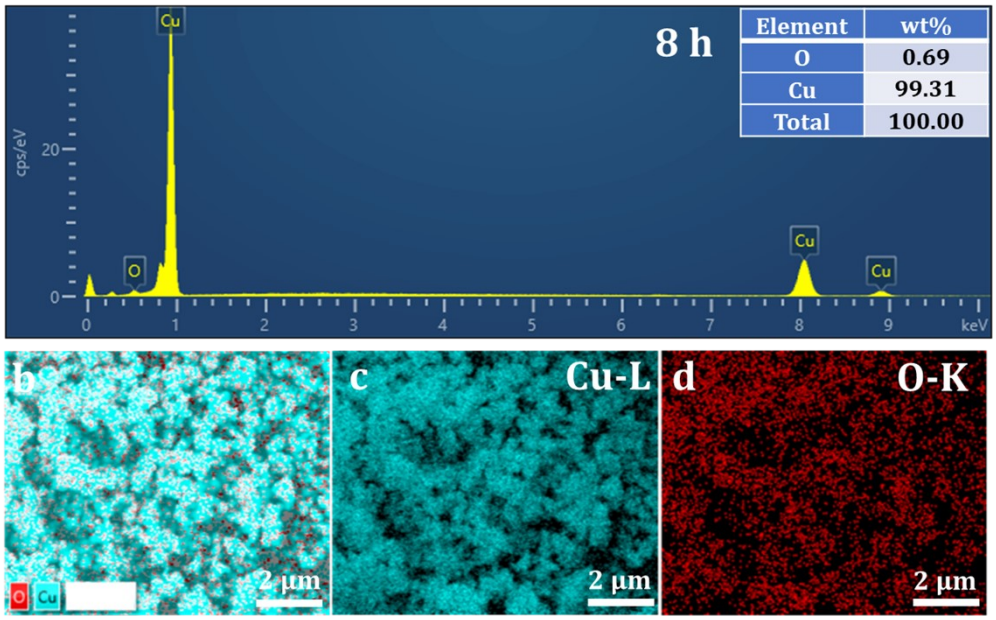

Figure S14. (a) EDS spectrum and (b-d) corresponding elemental distribution maps of P-8h sample.

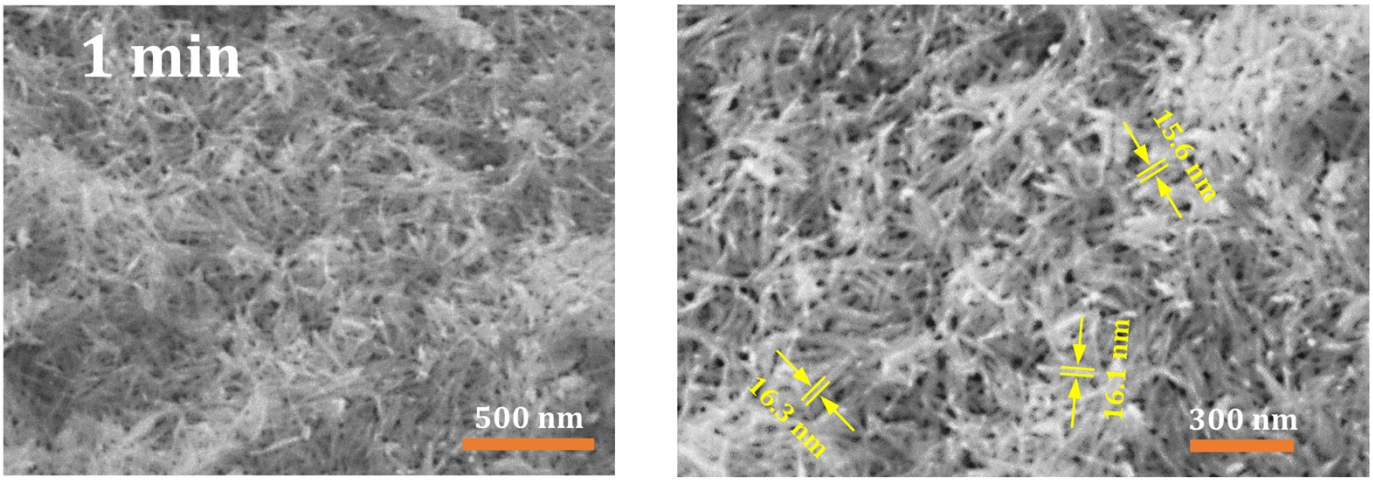

Figure S15. Low- and high-magnification FESEM images of P-1min.

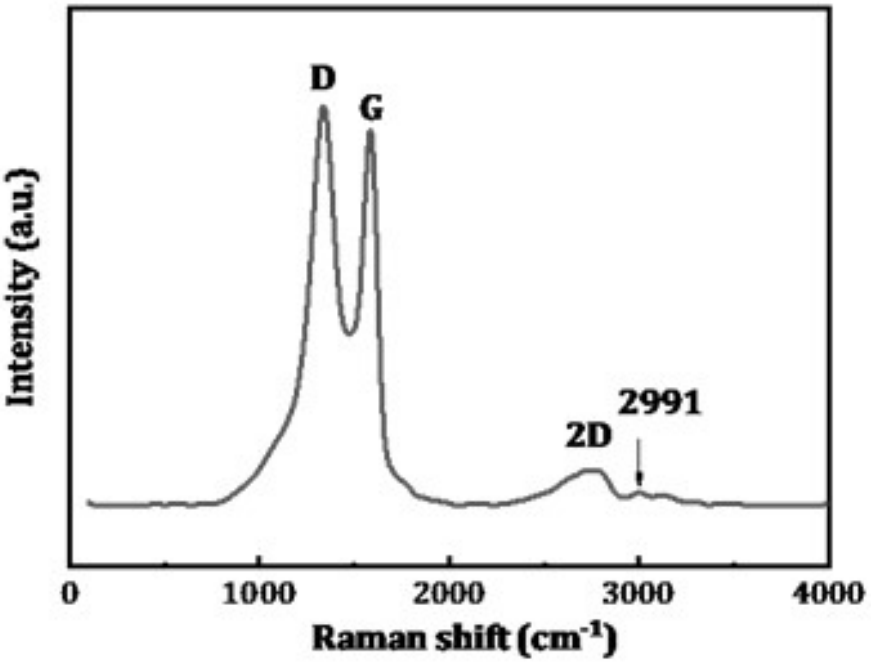

Figure S16. Raman spectrum of the P-1min sample.

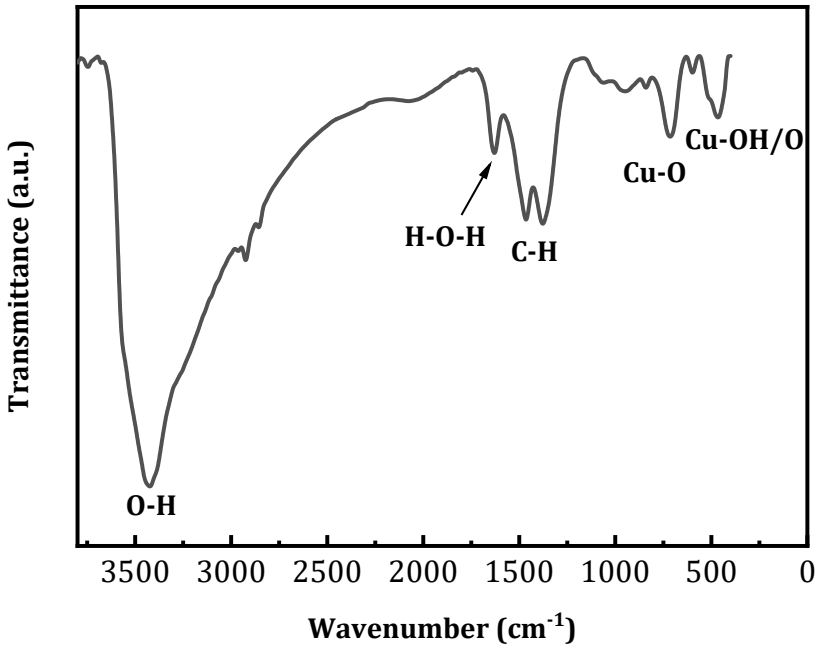

Figure S17. FTIR spectrum of the P-1min sample.

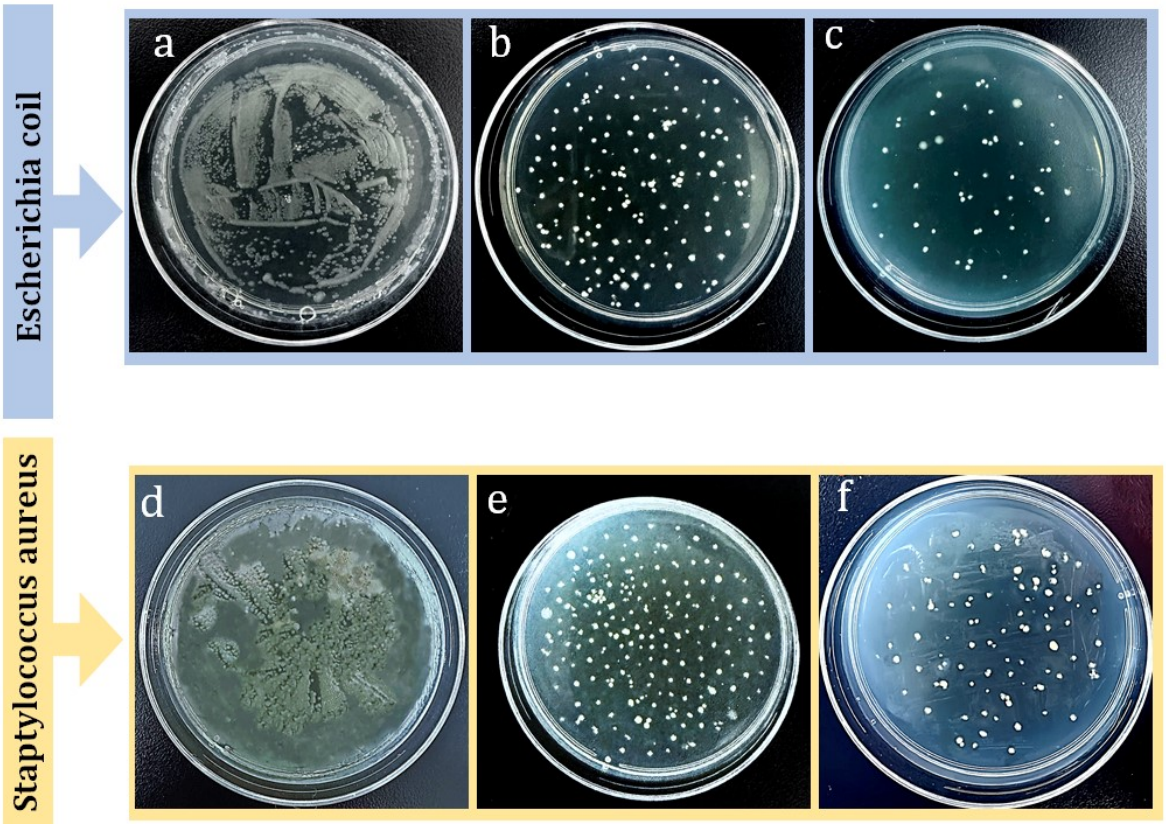

Figure S18. Concentration-dependent antibacterial activity of Cu/E6 NPs against *E. coli* and *S. aureus* after 12 h treatment: (a-c) *E. coli* treated with 0.05, 0.10, and 0.25 g L^{-1} Cu/E6 NPs, respectively; (d-f) *S. aureus* treated with 0.05, 0.10, and 0.25 g L^{-1} Cu/E6 NPs, respectively.

Figure S18 shows the concentration-dependent antibacterial activity of Cu/E6 NPs against Gram-negative bacterium *E. coli* and Gram-positive bacterium *S. aureus* at 0.05, 0.10, and 0.25 g L^{-1} after 12 h treatment. For *E. coli*, only weak antibacterial activity was observed at 0.05 g L^{-1} (Fig. S18a). When the concentration increased to 0.10 and 0.25 g L^{-1}, the number of viable colonies decreased markedly, with inhibition rates of 46.7% and 86.3%, respectively (Fig. S18b, c). For *S. aureus*, a similar concentration-dependent trend was observed. Limited inhibition was observed at 0.05 g L^{-1} (Fig. S18d), while the inhibition rates increased to 33.3% and 71.3% at 0.10 and 0.25 g L^{-1}, respectively (Fig. S18e, f). These results demonstrate the dose-dependent antibacterial activity of Cu/E6 NPs against both bacterial strains. In addition, under the same sublethal concentrations, *E. coli* showed higher sensitivity to Cu/E6 NPs than *S. aureus*.

Table S1. ICP-MS quantification of soluble copper released from Cu/E6 NPs and commercial copper powder in agar medium after 12 h incubation.

Sample	Soluble copper concentration (μg/mL)
Cu/E6 NPs	10.13
Commercial Cu powder	5.18

The soluble copper species released from Cu/E6 NPs and commercial Cu powder were quantified under the same agar-medium conditions used for the antibacterial assay. After 12 h incubation, the agar medium containing the copper samples was fragmented, dispersed in 100 mL of deionized water at 25 °C, stirred at 300 rpm for 5 min, and filtered to remove residual solid particles. The filtrate was then analyzed by ICP-MS. As shown in Table S1, Cu/E6 NPs generated a higher concentration of soluble copper species than commercial Cu powder, with values of 10.13 and 5.18 μg/mL, respectively. This result suggests that the enhanced antibacterial activity of Cu/E6 NPs may be partly associated with their greater release of soluble copper species under the tested agar-based conditions.

Table S2. Comparison of antibacterial performance of copper nanoparticles.

Test samples	Method of synthesis	Size/shape	Concentration	Test Method	Bacteria	Antimicrobial activity	Refs
Cu/E6 NPs	One-pot chemical reduction in Ethaline DES	94.6 nm/ quasi-spherical	50-500 µg/mL; Cu^{2+} release: 10.13 µg/mL after 12 h	Agar dilution	*S. aureus; E. coli*	Complete inhibition against both *S. aureus* and *E. coli* after 12 h; MIC: *S. aureus* 500 µg/mL; *E. coli* 500 µg/mL	This work
Commercial Cu powder	Atomization	0.2-0.55 µm/ spherical	500 µg/mL; Cu^{2+} release: 5.18 µg/mL after 12 h	Agar dilution	*S. aureus; E. coli*	Inhibition rates of 94.7% against *S. aureus* and 89.5% against *E. coli* after 12 h	This work
CuNPs (Bio)	Extracellular synthesis using *Bacillus licheniformis* CPJN13S supernatant	7.7-18.4 nm/ polygonal/hexagonal	100 µg/mL	Growth curve analysis (OD600)	*S. aureus*	Maximum growth inhibition of 43% at 27 h	[1]
Cu NPs	Chemical reduction	~5.3 nm/ quasi-spherical	32 µg/mL	CFU counting after 2 h contact	*S. aureus; E. coli*	*E. coli:* 99.9% reduction at ≥8 µg/mL; *S. aureus*: 86.3-98.0%	[2]
PDA–Cu NPs / PDA–Cu@PgelMA gradient hydrogel	PDA–Cu NPs synthesized by dopamine polymerization with Cu^{2+}; incorporated into GelMA hydrogel by UV polymerization	~150 nm/ spherical	100 µg/mL	Agar plate/CFU counting for planktonic bacteria; crystal violet staining for biofilm	*S. aureus; E. coli*	PDA–Cu NPs: >94% killing of *S. aureus* and >92% killing of *E. coli* after 1 h. Gradient hydrogel: ~45% inhibition of *S. aureus* biofilm and ~53% inhibition of *E. coli* biofilm	[3]
F. vulgaris-CuNPs	Green synthesis using Falcaria vulgaris leaf extract	20–25 nm/ nearly spherical	2000-8000 µg/mL	Broth dilution; agar well/disk diffusion	*S. aureus; E. coli*	Inhibited *S. aureus* at 4000 µg/mL and *E. coli* at 8000 µg/mL	[4]
Cu^0NPs	Chemical reduction	2-47 nm/ Quasi-spherical	100 µg/mL	Broth microdilution (CLSI); colony counting for	*S. aureus; E. coli*	99.85% inhibition (*S. aureus*), 99.94% (*E. coli*)	[5]
CuNPs	Biogenic synthesis using green alga Botryococcus braunii extract	10-70 nm/ cubical/spherical/elongated	100-250 µg/mL	Agar well diffusion; broth dilution assay	*S. aureus; E. coli*	MIC: 250 µg/mL for *E. coli* and *S. aureus*	[6]

CuNPs from Geranium extract	Green synthesis using Geranium extract	~5–8 nm/ mostly spherical	150-300 µg/mL	Nutrient agar plate inhibition test/MIC assay	*E. coli*	Complete inhibition of *E. coli* at 150 µg/mL	[7]
CuNPs from Opuntia ficus-indica extract	Green synthesis using Opuntia ficus-indica extract	~5–10 nm/ mostly spherical				Complete inhibition of *E. coli* at 350 µg/mL	
CuNPs@Tinospora cardifolia-coated cotton fabric	Green synthesis using Tinospora cardifolia leaf extract; one-	63.3 nm/ spherical	175-300 µg/mL	Turbidimetric assay; cup plate	*S. aureus; E. coli*	101% against *S. aureus* at 175 µg/mL; 74% against *E. coli* at 300 µg/mL	[8]
Cu NPs	Thermal decomposition	4-18 nm/ spherical	200-3200 µg/mL	Broth dilution/OD600 inhibition assay; agar plate	*S. aureus*	99% at 1600 µg/mL; 99.6% at 3200 µg/mL	[9]
CuNP-WS1	Cu nanoparticles fixed on cellulosic walnut shell material	15-22 nm/ Cu nanoparticles fixed on cellulosic walnut shell	62.5-4000 µg/mL	Broth macro-dilution	*S. aureus; E. coli*	MIC: ≥1000 µg/mL	[10]
CuNP-WS2	Cu nanoparticles fixed on cellulosic walnut shell material	60-80nm/ Cu nanoparticles fixed on cellulosic walnut shell	62.5-4000 µg/mL	Broth macro-dilution	*S. aureus; E. coli*	MIC: *S. aureus* 250 µg/mL; *E. coli* 500 µg/mL	[10]
CuNP-WS3	Cu nanoparticles fixed on cellulosic walnut shell material	Aggregated metallic nanoparticles fixed on cellulosic walnut shell	62.5-4000 µg/mL	Broth macro-dilution	*S. aureus; E. coli*	MIC: S. aureus 125 µg/mL; E. coli 250 µg/mL	[10]
Cu-NPs	Green synthesis using pink rose petal extract	~200 nm/ spherical	4-2048 µg/mL	MIC assay; well diffusion method	*E. coli (standard & MDR)*	64 µg/mL against standard *E. coli*; 1024 µg/mL against *MDR E. coli*	[11]
CCM-450	Spray drying + calcination (450°C)	1-5 µm/Cu particles on porous carbon microspheres	62.5-500 µg/mL	Broth dilution method; plate counting method	*S. aureus; E. coli*	MIC: 125-500 µg/mL for E. coli, 62.5-250 µg/mL for S. aureus. For CCM-450(5:1), inhibition rate: 97% against E. coli, 99.6% against S. aureus (24 h contact)	[12]

References:

[1] S. Rani, S. Dhankher, P. Kumar, P. Dahiya, K. Arora, A.S. Dang, P.J.F.i.N. Suneja, Biosynthesis, optimization, and characterization of CuNPs using Bacillus licheniformis CPJN13S and their antibacterial activity, 7 (2025) 1663115.

[2] U. Bogdanović, V. Lazić, V. Vodnik, M. Budimir, Z. Marković, S.J.M.l. Dimitrijević, Copper nanoparticles with high antimicrobial activity, 128 (2014) 75-78.

[3] J. Zhu, A. Wang, X. Miao, H. Ye, S. Pan, C. Zhang, Q. Qian, F.J.R.a. Su, Harnessing gradient gelatin nanocomposite hydrogels: a progressive approach to tackling antibacterial biofilms, 13 (2023) 30453-30461.

[4] M.M. Zangeneh, H. Ghaneialvar, M. Akbaribazm, M. Ghanimatdan, N. Abbasi, S. Goorani, E. Pirabbasi, A.J.J.o.P. Zangeneh, P.B. Biology, Novel synthesis of Falcaria vulgaris leaf extract conjugated copper nanoparticles with potent cytotoxicity, antioxidant, antifungal, antibacterial, and cutaneous wound healing activities under in vitro and in vivo condition, 197 (2019) 111556.

[5] L. Argueta-Figueroa, I. Álvarez-Solorza, A. Moreno-Rodríguez, N. Torres-Gómez, A.R. Vilchis-Nestor, J.L. García-Rivas, R.J.D.M. Torres-Rosas, Study of antibacterial and cytotoxic properties of copper nanoparticles obtained through a novel approach, 5 (2025) 231.

[6] A. Arya, K. Gupta, T.S. Chundawat, D.J.B.c. Vaya, applications, Biogenic synthesis of copper and silver nanoparticles using green alga Botryococcus braunii and its antimicrobial activity, 2018 (2018) 7879403.

[7] J. Bocarando-Chacón, D. Vargas-Vazquez, F. Martinez-Suarez, C. Flores-Juárez, M.J.A.P.A.M.S. Cortez-Valadez, Processing, Surface-enhanced Raman scattering and antibacterial properties from copper nanoparticles obtained by green chemistry, 126 (2020) 1.

[8] P. Sharma, S. Pant, V. Dave, K. Tak, V. Sadhu, K.R.J.J.o.m.m. Reddy, Green synthesis and characterization of copper nanoparticles by Tinospora cardifolia to produce nature-friendly copper nano-coated fabric and their antimicrobial evaluation, 160 (2019) 107-116.

[9] R. Betancourt-Galindo, P. Reyes-Rodriguez, B. Puente-Urbina, C. Avila-Orta, O. Rodríguez-Fernández, G. Cadenas-Pliego, R. Lira-Saldivar, L.J.J.o.N. García-Cerda, Synthesis of copper nanoparticles by thermal decomposition and their antimicrobial properties, 2014 (2014) 980545.

[10] T. Mehdizadeh, A. Zamani, S.M. Abtahi Froushani, Preparation of Cu nanoparticles fixed on cellulosic walnut shell material and investigation of its antibacterial, antioxidant and anticancer effects, Heliyon, 6 (2020).

[11] X. Yuan, Y. Wang, The Green Synthesis of Cu Nanoparticles and Investigation of the Antibacterial Properties and Cytotoxicity on Multidrug-Resistant E. coli, Curr. Top. Med. Chem., 26 (2025) 1004-1013

[12] X. Cheng, A. Fu, H. Li, Y. Wang, P. Guo, J. Liu, J. Zhang, X.S.J.A.S.C. Zhao, Engineering, Sustainable preparation of copper particles decorated carbon microspheres and studies on their bactericidal activity and catalytic properties, 3 (2015) 2414-2422.